ARTICLE

Regulation of invariant NKT cell development and function by a 0.14 Mbp locus on chromosome 1: a possible role for *Fcgr3*

Victoria L. DeVault[1,2] · Murisa Malagic[1] · Linda Mei[1] · Oliver Dienz[1] · Graham W. J. Lilley[1] · Patrick Benoit[1] · Somen K. Mistri[1,2] · Shawn C. Musial[1] · Jennifer L. Ather[3] · Matthew E. Poynter[2,3] · Jonathan E. Boyson [1,2]

Abstract
Invariant NKT (iNKT) cells are tissue-resident innate-like T cells critical to the host immune response. We previously identified a 6.6 Mbp region on chromosome 1 as a major regulator of iNKT cell number and function in C57BL/6 and 129X1/SvJ mice. Here, we fine-mapped this locus by assessing the iNKT cell response to alpha-galactosylceramide (αGalCer) in a series of B6.129 congenic lines. This analysis revealed the presence of at least two genetic elements that regulate iNKT cell cytokine production in response to αGalCer. While one of these genetic elements mapped to the B6.129c6 interval containing *Slam* genes, the dominant regulator in this region mapped to the 0.14 Mbp B6.129c3 interval. In addition, we found that numbers of thymic iNKT cells and DP thymocytes were significantly lower in B6.129c3 mice, indicating that this interval also regulates iNKT cell development. Candidate gene analysis revealed a fivefold increase in *Fcgr3* expression in B6.129c3 iNKT cells, and we observed increased expression of FcγR3 protein on B6.129c3 iNKT cells, NK cells, and neutrophils. These data identify the B6.129c3 interval as a novel locus regulating the response of iNKT cells to glycosphingolipid, revealing a link between this phenotype and a polymorphism that regulates *Fcgr3* expression.

Introduction

Semi-invariant iNKT cells comprise an unusual innate-like T cell subset that has significant roles in the host immune response to bacterial and viral pathogens [1–3]. iNKT cells recognize glycolipids and glycosphingolipids presented by the MHC class I-like molecule CD1d [4–6]. The prototypical glycosphingolipid agonist alpha-galactosylceramide (αGalCer) is structurally similar to glycosphingolipids from *Bacteroides fragilis* [7] and is a potent activator of iNKT cells [6, 8–11]. Upon activation by αGalCer presented by CD1d, iNKT cells rapidly produce large amounts of chemokines and cytokines [12–14] and contribute to an orchestrated activation of both innate and adaptive immune cells including dendritic cells, macrophages, and natural killer (NK) cells [15–19]. The iNKT cell subset, therefore, is uniquely poised to shape the quality and magnitude of the developing host immune response.

Invariant NKT cell number and function varies markedly among mice of different genetic backgrounds. Wild-derived inbred strains (e.g., PWD/PhJ, Cast/EiJ) have barely detectable numbers of iNKT cells [20, 21], and there is significant strain-dependent variability even among common laboratory inbred strains [21–25]. Accumulating evidence suggests that the genetic background has a significant influence on the role of iNKT cells in the host immune response. For example, iNKT cells are critical in the clearance of the opportunistic pathogen *Pseudomonas aeruginosa* from the lung in BALB/cJ mice, but are dispensable in C57BL/6J mice [26]. Similarly, pathology in

✉ Jonathan E. Boyson
jboyson@uvm.edu

[1] Department of Surgery, University of Vermont Larner College of Medicine, Burlington, VT, USA

[2] Cellular, Molecular, and Biomedical Sciences Program, University of Vermont, Burlington, VT, USA

[3] Division of Pulmonary Disease and Critical Care, Department of Medicine, Vermont Lung Center, University of Vermont Larner College of Medicine, Burlington, VT, USA
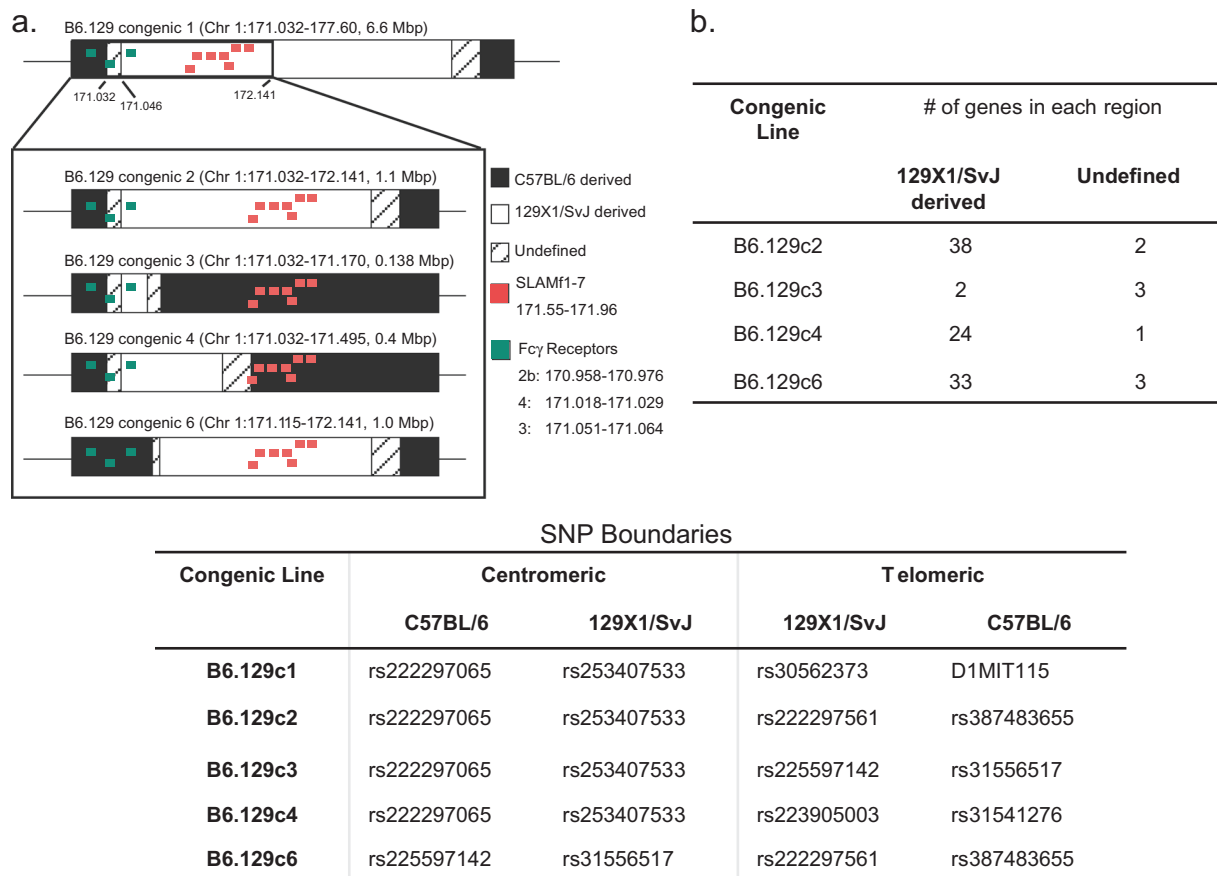
Fig. 1 Fine-mapping of the B6.129c1 congenic interval. **a** *Left:* Schematic of the chromosome 1 congenic intervals used in this study. Black regions denote C57BL/6 derived regions, white denotes 129X1/SvJ derived regions, and the cross-hatched region is either C57BL/6 or 129X1/SvJ derived (undefined). For reference, the *Slam* family genes are denoted in red and the Fc receptor gene family is denoted in green. **b** Number of protein-coding genes predicted in each subcongenic interval. *Lower:* Reference SNPs that define boundaries for each congenic line on the centromeric and telomeric ends

iNKT cell-deficient mice infected with *Borrelia burgdorferi* manifests as joint inflammation in BALB/c mice [27] and as myocarditis in C57BL/6J mice [28]. Therefore, a thorough understanding of the genetic determinants that regulate iNKT cell development and function is necessary to understand the role of iNKT cells in the host immune response.

Numerous reports have described polymorphic genetic loci that regulate iNKT cell number and function [20, 29–35]. We and others have identified a region on chromosome 1 that regulates iNKT cell development and the response to αGalCer [25, 29, 31, 36]. We previously demonstrated that iNKT cells in 129X1/SvJ mice produced significantly lower amounts of cytokine after αGalCer challenge than did iNKT cells in C57BL/6J mice. Using B6.129 congenic mice, we identified the genetic interval spanning from D1MIT270 to D1MIT115 (Chr1: 170.84–177.68 Mbp) as a regulator of the response of iNKT cells to in vivo αGalCer challenge [31]. This ~6.6 Mbp locus is densely populated with numerous

immunologically relevant genes, including signaling lymphocyte activation markers (SLAMs) that modulate iNKT cell development and function [37]. Interestingly, this locus overlaps extensively with several autoimmune susceptibility loci [38–40] and there are numerous reports of an association between iNKT cell numbers and autoimmunity [25, 41–43].

To refine this interval and identify candidate genes that regulated the responsiveness of iNKT cells to αGalCer, we generated additional B6.129 subcongenic lines with overlapping intervals. Here, we report the mapping of the iNKT cell response to αGalCer to a minimal 0.14 Mbp interval (Chr1: 171.032–171.170) containing 4 genes and 2 microRNAs. In addition, we found that this interval regulates total thymocyte numbers and total iNKT cell number. Finally, we identify *Fcgr3* as a possible candidate iNKT cell regulatory gene due to the association of increased iNKT cell FcγR3 expression and impaired response of iNKT cells to αGalCer stimulation observed in B6.129c3 mice.
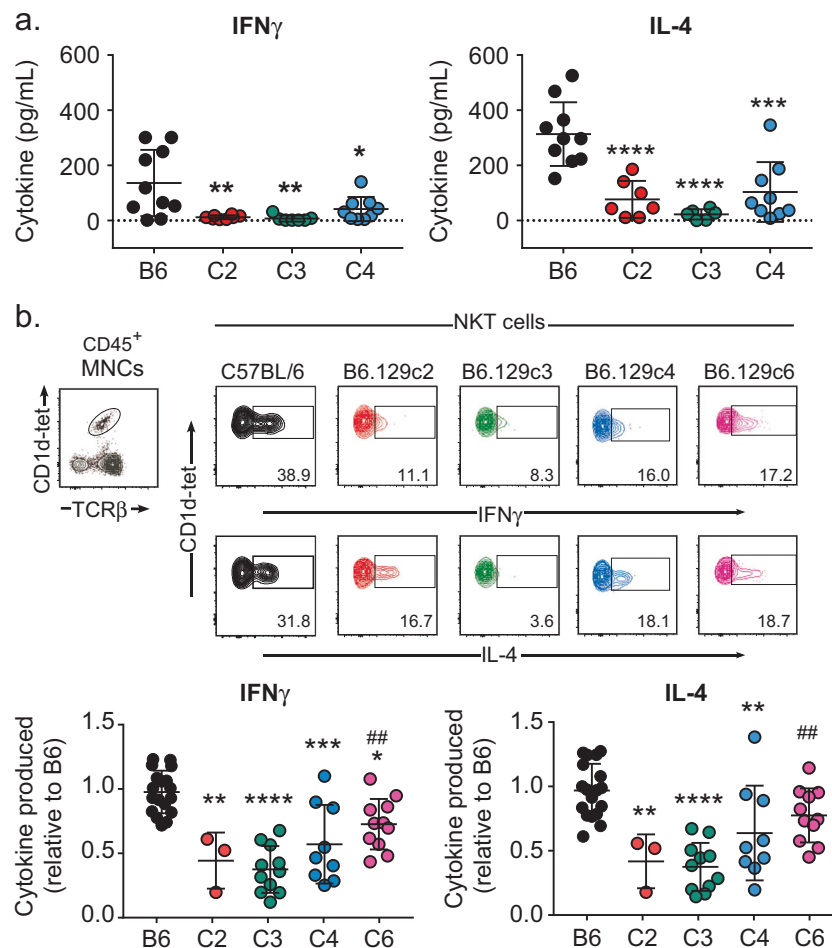
Fig. 2 Regulation of αGalCer-induced iNKT cell cytokine production maps to a 0.14 Mbp region on chromosome 1. **a** Decreased serum cytokine in B6.129 congenic mice in response to αGalCer. Blood was collected from B6 or B6.129 congenic mice 2 h after αGalCer administration. Serum cytokine levels were assessed using ELISA. Statistical analysis was performed using one-way ANOVA followed by Sidak's multiple comparisons test, $*p \leq 0.05$, $**p \leq 0.01$, $***p \leq 0.001$, $****p \leq 0.0001$. **b** *Top:* Representative intracellular staining of cytokine-producing iNKT cells in response to αGalCer. Splenocytes were isolated 2 h after αGalCer administration. iNKT cells were identified using CD1d-tetramer/PBS57 and TCRβ. The percentages of iNKT cells expressing cytokines were determined using an isotype control for each mouse. *Lower:* Decreased iNKT cell cytokine production in B6.129 congenic mice in response to αGalCer. The data represent the relative level of iNKT cell cytokine production. Data are the combined data from five separate experiments using female mice 8–14 weeks of age and are presented as the mean ± s.d. All mice were age-matched to controls in each experiment. Statistical analysis was performed using 2-way ANOVA followed by Tukey's multiple comparison test. * = comparison of B6 to B6.129 congenics. # = comparison of B6.129c3 to B6.129 congenics. $*p \leq 0.05$, $**,$ $\#\#p \leq 0.01$, $***p \leq 0.001$, $****p \leq 0.0001$

Results

Refinement of the 129X1/SvJ interval on chromosome 1

We previously reported that a 6.6 Mbp genetic region on chromosome 1 containing the *Slam* genes regulated iNKT cell function [31]. Given previous reports that SLAMf1 and SLAMf6 are required for iNKT cell development and the *Slam* genes have been reported to regulate thymic iNKT cell numbers [31, 44], we hypothesized that polymorphisms in one or more of the *Slam* genes are responsible for the differences in the iNKT cell response to αGalCer between C57BL/6 and 129X1/SvJ mice. To test this hypothesis, we generated 4 subcongenic strains: B6.129c2, B6.129c3, B6.129c4, and B6.129c6 with overlapping 129X1/SvJ intervals ranging from 0.14 Mbp to 1.1 Mbp that spanned the centromeric region of the B6.129c1 interval containing *Slam* family genes (Fig. 1a). Mapping of the 129 derived-interval boundaries (Fig. 1b) revealed that B6.129c2 and B6.129c6 strains possess *Slam* family genes derived from 129X1/SvJ, while B6.129c3 and B6.129c4 strains possess *Slam* family genes derived from C57BL/6J.
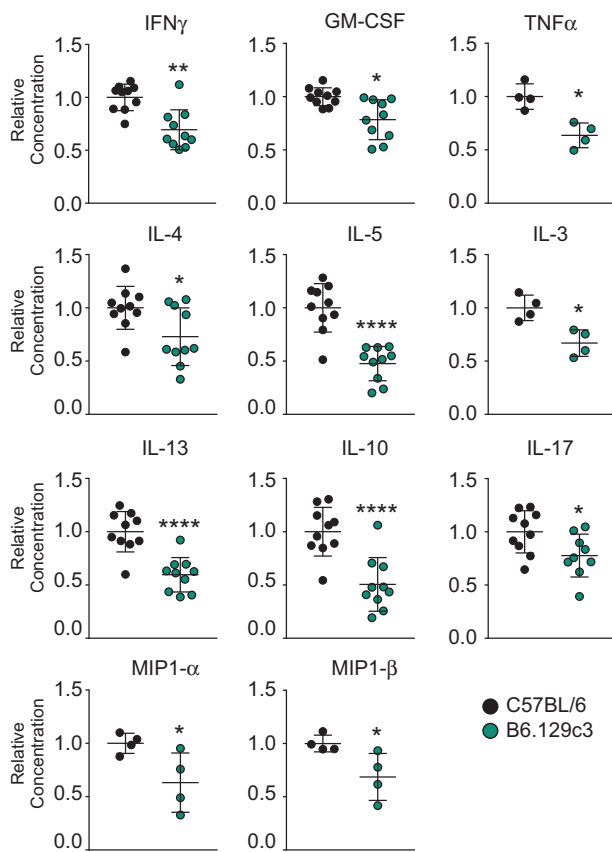
Fig. 3 Reduced cytokine production in B6.129c3 is iNKT cell-intrinsic. iNKT cells were sorted from C57BL/6 or B6.129c3 splenocytes. Cells were stimulated using anti-CD3 and anti-CD28 for 72 h, after which supernatants were analyzed using Milliplex. Data represent the cumulative results from three separate experiments using 8–11 week-old female mice. Mice were age-matched in each experiment. Statistical analysis was performed using a two-way ANOVA followed by the Holm–Sidak multiple comparison test and is reported as the mean normalized concentration ± s.d. *$p \leq 0.05$, **$p \leq 0.01$, ****$p \leq 0.0001$

Invariant NKT cell cytokine production in response to αGalCer maps to a 0.14 Mbp region on chromosome 1

To determine which 129X1/SvJ intervals regulated the iNKT cell response to glycolipid, we assessed serum IFN-γ and IL-4 cytokine levels after administration of αGalCer to C57BL/6 and B6.129 congenic strains. This analysis revealed that each of the tested B6.129 congenic strains exhibited significantly reduced levels of serum cytokines in comparison to the B6 control (Fig. 2a). To determine whether this decrease in αGalCer-induced cytokine was due to reduced production by iNKT cells, we evaluated IFNγ and IL-4 production by CD1d-tetramer/PBS57-gated cells in response to αGalCer using intracellular flow cytometry staining (Fig. 2b). Consistent with the reduced serum cytokine production in the B6.129 congenic strains in

response to αGalCer administration, we observed significantly lower levels of iNKT IFN-γ and IL-4 production in B6.129c2, B6.129c3, and B6.129c4 strains as compared to the B6 parental strain (Fig. 2b). These data indicated that the dominant regulator of iNKT cell cytokine production in response to αGalCer mapped to the minimal 0.14 Mbp B6.129c3 interval.

Interestingly, examination of the cytokine production in B6.129c6 mice revealed an intermediate phenotype. iNKT IFN-γ and IL-4 production in B6.129c6 mice were significantly higher in comparison to B6.129c3 mice, while B6.129c6 IFN-γ was significantly lower in comparison to B6 parental mice (Fig. 2b). B6.129c6 IL-4 was also lower than B6 mice, although this reduction did not reach statistical significance ($p = 0.0880$) (Fig. 2b). Together, these data indicated the presence of at least two genetic elements in the B6.129c2 region that regulate iNKT cell cytokine production in response to αGalCer: a dominant regulator mapping to the 0.14 Mbp B6.129c3 interval that did not contain *Slam* genes, and a second subdominant regulator mapping to the B6.129c6 interval containing *Slam* genes.

Differences in in vivo iNKT cell cytokine production could be the result of an iNKT cell-intrinsic phenomenon, or from differences in antigen processing and presentation. To determine whether the difference in iNKT cell cytokine production was an iNKT-intrinsic phenomenon, we directly compared cytokine production from purified B6 and B6.129c3 iNKT cells after stimulation. Equal numbers of sorted splenic iNKT cells from B6 WT and B6.129c3 mice were stimulated with anti-CD3 and anti-CD28, after which supernatants were analyzed for cytokine and chemokine production. We observed a significant reduction in cytokines and chemokine secretion from B6.129c3 iNKT cells compared to their B6 counterparts (Fig. 3). Taken together, these data indicate that one or more of the genes contained within the B6.129c3 interval regulates iNKT cell cytokine production through an iNKT-intrinsic process.

Reduced numbers of thymic iNKT cells in B6.129c3 mice

Since it has been previously reported that the *Nkt1* locus which encompasses the B6.129c3 congenic interval, regulates thymic iNKT cell number [29], we asked whether this phenotype could be mapped to the B6.129c3 interval. A comparison of thymic iNKT cell numbers revealed a significant reduction in B6.129c3 thymic iNKT cells compared to their B6 counterparts (Fig. 4a). Further analysis revealed that there was no significant difference in the overall frequency of thymic iNKT cells (data not shown), and that the decrease in thymic iNKT cell number in B6.129c3 mice was associated with a decrease in total thymocyte number (Fig. 4a). Specifically, we observed a specific decrease in
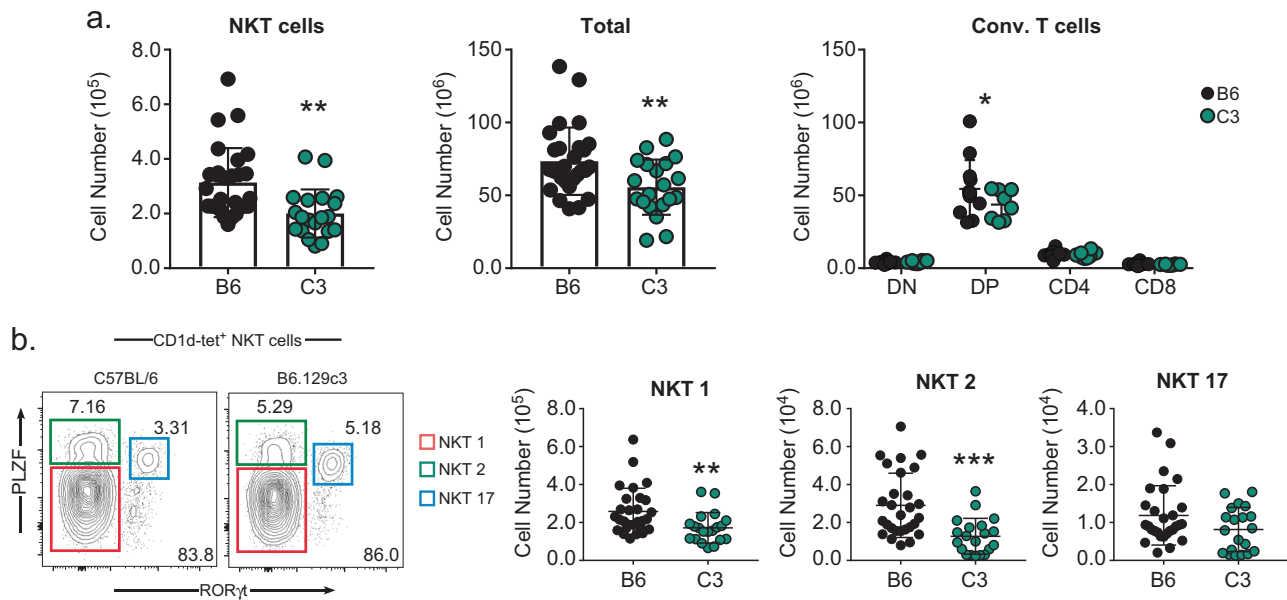
Fig. 4 iNKT cell numbers in the thymus are regulated by the B6.129c3 interval. **a** iNKT cell (*left*), total thymocyte (*middle*), and thymocyte subset (*right*) numbers were compared between C57BL/6 and B6.129c3 mice. **b** No significant difference in the distribution of thymic iNKT subsets between B6 and B6.129c3 mice. iNKT cell subsets were identified based on PLZF and RORγt expression as indicated by colored boxes (*left*). Cumulative numbers of iNKT cell subsets are shown (*right*). Data represent the cumulative results of 4 separate experiments using 9–13-week-old female mice. Mice were age-matched in each experiment. Statistical analysis was performed using an unpaired *t*-test. *$p \leq 0.05$, **$p \leq 0.01$, ***$p \leq 0.001$

the number of DP, but not DN, CD4 or CD8 SP, B6.129c3 thymocytes. These data suggest that the B6.129c3 interval indirectly regulates iNKT cell development through its influence on the DP stage of thymocyte development.

Accumulating data suggest that there is significant strain-dependent variation in the distribution of iNKT cell subsets [23, 45]. Therefore, we considered the possibility that the iNKT cell-intrinsic differences in cytokine production was due to regulation of the distribution of iNKT cell subsets by the B6.129c3 congenic interval. iNKT1, iNKT2, and iNKT17 subsets were identified according to their expression of PLZF and RORγt [45] (Fig. 4b, left). Examination of the frequency and number of thymic iNKT cell subsets in C57BL/6 and B6.129c3 mice revealed a decrease in the numbers of iNKT1 and iNKT2 cells, consistent with the decrease in total iNKT cell numbers (Fig. 4b). The iNKT17 subset also showed a trend toward lower numbers in the B6.129c3 mouse, albeit not significantly lower. Taken together, these results suggest that the B6.129c3 interval regulates the number of thymic iNKT cells but does not significantly affect the distribution of iNKT cell subsets.

Increased expression of FcγR3 on B6.129c3 iNKT cells

The B6.129c3 congenic interval contains 4 genes and two microRNAs (Table 1). Examination of gene expression data

using the Immgen database [46] suggested that one of the genes, *Mpz* (myelin protein zero) is not expressed in leukocytes, and we confirmed this data using PCR and gene-specific primers (data not shown).

We next investigated whether one or more of the remaining three genes, *Fcgr3* (Fc fragment of IgG receptor III), *Cfap126* (cilia and flagella-associated protein), or *Sdhc* (succinate dehydrogenase complex c), were differentially expressed in B6.129c3 naive mice compared to C57BL/6 controls. We sorted splenic iNKT cells from C57BL/6 and B6.129c3 mice and used quantitative PCR to assess gene expression. Interestingly, we found that *Fcgr3* gene expression was significantly higher (5.5-fold change) on B6.129c3 iNKT cells compared to their B6 counterparts (Fig. 5a). In contrast, no significant differences in *Cfap126* or *Sdhc* expression were observed between the two strains.

We next determined whether the increase in *Fcgr3* gene expression correlated with an increase in protein expression on the surface of B6.129c3 iNKT cells. Similar to a previous report [47], we observed a very low, but detectable level of FcγR3 expression on naïve iNKT cells from B6.129c3 mice as well as from parental strain 129X1/SvJ mice (Fig. 5b). To confirm the increased expression of FcγR3 in B6.129c3 mice, we also assessed expression on neutrophils which express significant levels of this protein. This analysis similarly revealed increased FcγR3 expression on neutrophils from both B6.129c3 and 129X1/SvJ parental

Table 1 Genetic elements within the B6.129c3 interval

Gene	Name	Position	Non-synonymous SNPs
Fcgr3	Fc receptor IgG, low affinity III	171.051–171.064	12
Cfap126	Cilia and flagella-associated protein	171.113–171.126	1
Mpz	Myelin Protein Zero	171.150–171.161	1
Sdhc	Succinate Dehydrogenase Complex Subunit C	171.127–171.150	2
Mir6546 GM27844	microRNA	171.064–171.079	n.a.

Gene positions were determined according to Ensembl release 90. Structural variants, missense variants, and splice variants were determined using the Mouse Phenome Database, Sanger 4, and NCBI dbSNP databases. SNP values are those that result in amino acid changes between C57BL/6 and 129S1/SvImJ. The B6.129c3 interval boundaries are on chromosome 1 location 171.032 to 171.170 Mbp

mice (Fig. 5b). We then compared iNKT FcγR3 expression between αGalCer-treated B6 and B6.129c3 mice to determine if activation altered the relative expression. While this analysis revealed significantly greater FcγR3 on iNKT cells and NK cells, the relative expression difference was similar to that seen in naïve mice (Fig. 5c). Together, these data suggest that one or more polymorphisms in the B6.129c3 interval regulates *Fcgr3* gene and cell surface expression, and identifies *Fcgr3* as a candidate gene responsible for regulation of the iNKT cell responsiveness to αGalCer.

Discussion

The ability of iNKT cells to rapidly produce large amounts of cytokines and chemokines in response to pathogens puts them in a unique position to shape the developing host immune response. In this context, natural genetic variants that modulate iNKT cell function could have significant downstream effects on the host immune response to pathogens. We recently demonstrated that two seemingly conflicting reports regarding the role of iNKT cells in the clearance of *Pseudomonas aeruginosa* from the lung [48, 49] could be reconciled when genetic background was taken into consideration [26]. For reasons that are still unclear, BALB/c iNKT cells make a significant contribution to the host immune response after *P. aeruginosa* infection, but B6 iNKT cells do not. The strain-dependent role of iNKT cells in bacterial clearance was associated with strain-dependent differences in the response of lung iNKT cells to αGalCer. Elucidation of genetic variants that regulate iNKT cell function is necessary to understand their role in the host immune response.

Invariant NKT cell number, function, and tissue-specific homing varies widely among inbred strains of mice [22, 23, 31, 45] and several polymorphic loci that regulate iNKT cell number have been identified [20, 25, 29, 31, 32, 36, 43, 50].

In an investigation into the role of iNKT cells in type 1 diabetes, it was reported that autoimmune-prone non-obese diabetic (NOD) mice possessed very low numbers of iNKT cells [25, 41, 51]. A genetic locus, *Nkt1*, regulating the number of thymic iNKT cells was identified and mapped to a distal region on chromosome 1 (D1MIT15 - D1MIT155). The *Nkt1* locus contained several immunologically relevant genes including, *CD247, FcγR2b, FcγR3*, and the *Slam* family of receptors including *Slamf1* and *Slamf6* [30, 36], which are required for iNKT cell development in the thymus [37]. A subsequent report implicated *Slamf1* in the regulation of thymic iNKT cell numbers as well as iNKT IL-4, but not IFN-γ, production [29]. Here, we have refined this locus further and have found evidence suggesting the presence of at least two regulators of NKT cell number and function. Our data suggest that *Slam* genes may not be the major regulators of the iNKT cell response to αGalCer in this region. Although B6.129c6 mice that possess the *Slam*[129] and *Fcgr*[B6] alleles exhibited reduced IFN-γ and IL-4 production in comparison to B6 mice, the dominant effect was observed in B6.129c3 and B6.129c4 mice that possess *Slam*[B6] and *Fcgr*[129] alleles. Conversely, the observation that B6.129c6 iNKT cell cytokine production was significantly greater than their B6.129c3 counterparts in both cytokines measured is consistent with the presence of an additional gene or genetic modifier regulating this phenotype. Together, these data suggest the possibility that there are multiple genetic elements in the larger B6.129c2 interval that regulate the function of iNKT cells: a novel genetic element that we identified in the B6.129c3 interval, and one or more genes (most likely *Slam* genes) or genetic modifiers in the B6.129c6 interval.

We identified *Fcgr3* as a candidate gene in regulating the iNKT cell response. FcγR3 (CD16) is an activating receptor that binds IgG and signals through an immune-tyrosine activation domain (ITAM) and is highly expressed on
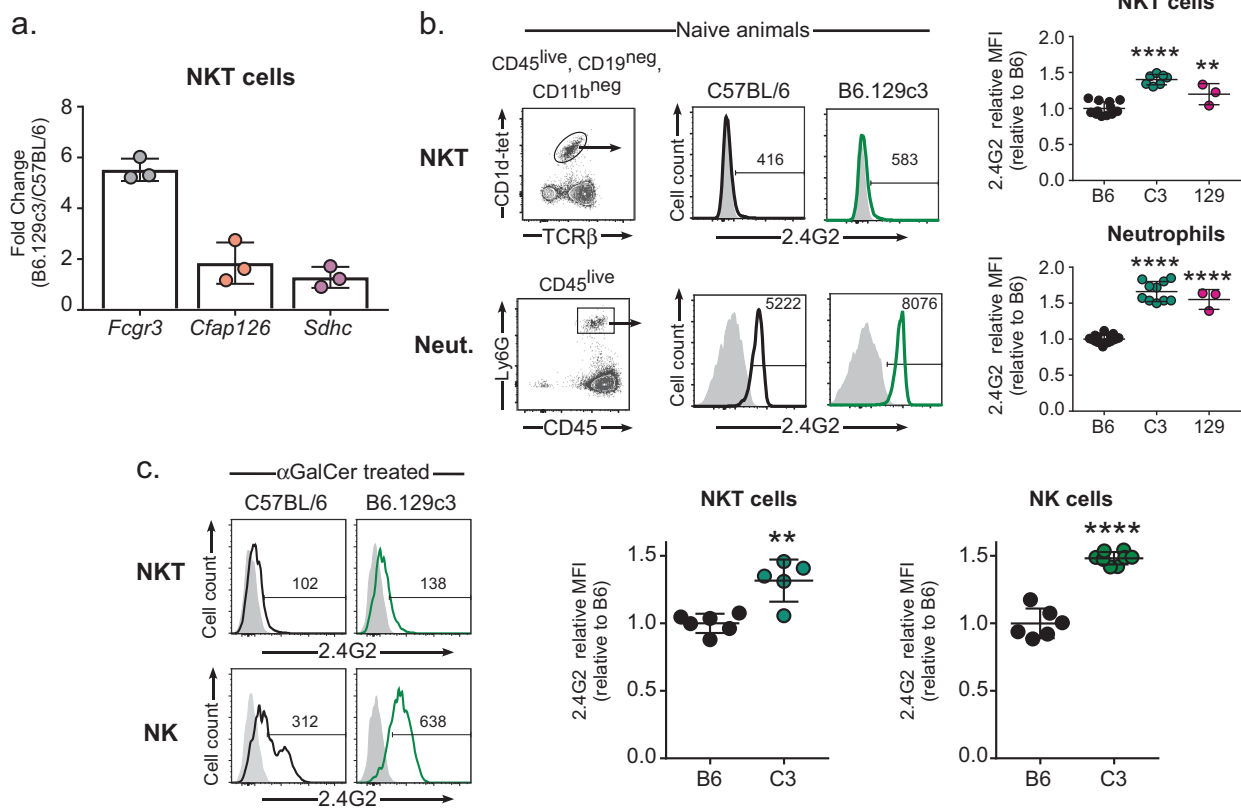
Fig. 5 Increased *Fcgr3* gene and protein expression on B6.129c3 iNKT cells. **a** Increased *Fcgr3* gene expression in B6.129c3 splenic iNKT cells. Spleen iNKT cells were sorted using CD1d-tetramer/PBS57 for RNA isolation. Gene expression was determined using quantitative PCR. Data are reported as the fold change relative to B6. **b** Increased cell surface protein expression of FcγR3 on naive B6.129c3 iNKT and neutrophils. Representative flow cytometry histograms show expression levels of FcγR3 on B6.129c3 iNKT cells (*upper*) and neutrophils (*lower*). Shaded dark histograms represent cells blocked with unconjugated 2.4G2 Ab and subsequently stained with conjugated isotype control. Heavy lined histograms are cells stained with conjugated 2.4G2 Ab. The numbers represent the median fluorescence intensity (MFI). Graphs depict the normalized MFI of 2.4G2 relative to the B6 control. Data represent the mean ± s.d. and is the cumulative data from two separate experiments of female mice aged 6–8 weeks. **c** Increased cell surface protein expression of FcγR3 on αGalCer-treated B6.129c3 iNKT and NK cells. Shaded dark histograms represent cells blocked with unconjugated 2.4G2 Ab and subsequently stained with conjugated isotype control. Heavy lined histograms are cells stained with conjugated 2.4G2 Ab. The numbers represent the median fluorescence intensity (MFI). Graphs depict normalized MFI of 2.4G2 relative to the B6 control. Data represent the mean ± s.d. and is representative data from two independent experiments using 10 or 14-week-old female mice. Statistics were performed using an unpaired *t*-test. $**p \leq 0.01$, $****p \leq 0.0001$

monocytes, macrophages, neutrophils, and NK cells [47, 52]. We found that FcγR3 gene and protein expression was significantly increased on iNKT cells, NK cells, and neutrophils in B6.129c3 and 129X1/SvJ parental mice compared to C57BL/6 controls. The underlying basis for this differential expression is still unclear. A comparison of *Fcgr3* promoter sequence (as defined by the Eukaryotic promoter database [53]) between C57BL/6 and 129S1/SvImJ strains revealed no nucleotide differences. However, over 100 upstream variants were identified, suggesting the possibility that a substitution in an enhancer element could affect expression (data not shown).

Here, we confirm previous reports that iNKT cells express low, but detectable levels of FcγR3 [47, 54, 55]. These previous reports demonstrate that engagement of Fc receptors can significantly modulate iNKT cell function. In one study, intravenous Ig (IVIG) treatment was found to exert some of its effect through its action on iNKT cells [54], and IVIG administration to C57BL/6 mice resulted in diminished iNKT cell activation. Co-administration of αGalCer and IVIG resulted in severely reduced IL-4 and IFN-γ production compared to mice treated with αGalCer alone, and this inhibition was dependent on FcγR3 [55]. Our finding that increased expression of FcγR3 on B6.129c3 iNKT cells is associated with decreased cytokine production is consistent with these data, although it remains unclear whether there is increased FcγR3 signaling in B6.129c3 iNKT cells.

Given the association of increased *Fcgr3* in B6.129c3 mice and alterations in thymocyte number, it is possible that

Table 2 Primers for each SNP used in genotyping B6.129 congenic mice

SNP	Forward primer 5′–3′	Reverse primer 5′–3′
rs222297065	ACCGGACCATCTAGTGCATT	TCAGCACCTACTGGCACATT
rs253407533	ACTGGAGGTGAGGACACAGACA	ATGGTCCTTGGCTCTCCTTATG
rs222297561	CGCTCTGTTGGTTACTCTGAAG	AGAAGAGGCACACTGAGTAGGA
rs387483655	CCAGCCAAGTTATTAGGTTCAG	CAGGTGGTTCAGATCGATTACA
rs239276905	ACCATTGGCTGAAGAGTCTG	GAAGCTGCCAAGTTCTGCTA
rs8240241	CAGAAGACAACCAGCAGAAG	CGAATAGGACTCTCGCTGTA
rs223905003	TGGTGGCCATTAGTCACTCTTC	GAGCAATGACCATCAGACCTAT
rs31541276	AACACATGGTGGCTGACAAC	CAGTCTAGCAGGACTTAAGG
rs237951232	CCATCCTCTCACCCTTCACT	GGGCTTTCTAACTGCTCCTC
rs31556517	CTTGTTCTTCCTGCCTACAC	TGTCTGCCTGGAACACTCTT

All SNPs were identified using the Ensembl Gene annotation system, release 90 [68]

the NKT cell-intrinsic changes in function stem from differences in development. FcγR3 is expressed on developing thymocytes [56, 57] and *Fcer1g*, which encodes the signaling chain of FcγR3 contributes to TCR signaling [58, 59]. Interestingly, *Fcer1g* was recently demonstrated to be over-expressed in NKT1 cells, and deletion of *Fcer1g* resulted in altered frequencies of NKT1 and NKT2 subsets [60]. Whether the impaired iNKT cell function observed in B6.129c3 mice is associated altered FcγR3 and/or Fcεr1γ signaling will require further study.

Although our results suggest a role for *Fcgr3* in the regulation of iNKT cells, we cannot rule out the other genetic elements that lie within the B6.129c3 region. We did not see differences in gene expression of *Sdhc* or *Cfap126* genes on sorted splenic iNKT cells. Mutations in the *Sdha*, *b*, and *c* genes have been linked to susceptibility to mitochondrial disorders [61]. *Cfap126* has been shown to have a function on pancreatic β cells [62], but studies of this gene on iNKT cells have not been performed. Several microRNAs have had reported roles in regulating iNKT cell development, including the Let-7 family of microRNAs [63–65]. The microRNA Mir6546 present in the B6.129c3 interval appears to be rare [66, 67] and its function has not been studied in immune cells. Therefore, although this interval contains multiple genes and genetic elements, the most likely iNKT cell regulator within our interval is *Fcgr3*.

In summary, we have fine-mapped a locus that regulates the iNKT cell response to the agonist glycolipid αGalCer. Our findings suggest that the previously described *Nkt1* locus contains at least two genetic elements that regulate NKT cell number and function, and that the dominant regulator in the region maps to a congenic interval containing *Fcgr3*, identifying it as a probable candidate gene for these phenotypes. Further characterization of this genetic locus and of the Fc receptor signaling pathway will aid in our understanding of the role of iNKT cells in host immunity.

Materials and methods

Mice and reagents

C57BL/6J mice were purchased from The Jackson Laboratory (Bar Harbor, ME) and were bred at the University of Vermont. B6.129c1 mice were described previously [38]. B6.129c2, B6.129c3, B6.129c4, and B6.129c6 strains were generated by backcrossing B6.129c1 mice to C57BL/6J mice, and intercrossing the heterozygous progeny. Offspring in which recombinants were identified were backcrossed B6 to allow for the generation of homozygous congenic lines. The congenic interval boundaries were determined using primer sets designed to amplify across informative insertions/deletions and SNPs (Table 2). PCR products were sequenced to confirm boundaries. All mice were age and sex matched as indicated in the figure legends. Mice were housed in the specific pathogen-free barrier facility at the University of Vermont. The alpha-galactosylceramide (Avanti Polar Lipids, Alabaster, Alabama) was prepared as described previously [31] and administered i.p. at indicated doses in a 100 μL volume. All procedures involving animals were approved by the University of Vermont Institutional Animal Care and Use Committee.

Serum cytokine analysis

Mice were bled via cardiac puncture, after which serum was collected and frozen at −20 °C until analysis by ELISA according to the manufacturer's instructions (Biolegend, San Diego, CA, BD Biosciences, Franklin Lakes, NJ).

Flow cytometry

Splenocytes and thymocytes were obtained by gently pressing through a 70 μm nylon mesh. RBC's were lysed using Gey's solution. Cells were stained at 4 °C in PBS +

2% FBS containing 0.2% sodium azide for 30 min., after which they were washed and resuspended in PBS + 1% PFA. Abs used in these experiments were anti-CD4 (RM4-5), CD45 (30-F11), TCRβ (H57-597), NK1.1 (PK136), CD8 (53-6.7) (Biolegend), and CD11b (M1/70), CD16/32 (2.4G2), and CD19 (6D5) (BD Biosciences). UV Live Dead staining reagent was included in all experiments (Life technologies, ThermoFisher, Grand Island, NY). CD1d-tetramer loaded with PBS57 was provided by the National Institutes of Health (NIH) tetramer facility (Emory University Vaccine Center, Atlanta, GA).

For intracellular cytokine staining (ICS), cells were isolated from the spleen as described above and stained with Ab to surface markers. In every ICS experiment, cells were analyzed directly ex vivo without further treatment. After washing in staining buffer, cells were fixed with 4% PFA for 30 min at 4 °C. After washing in permeabilization buffer (0.1% saponin, 1% FCS, 0.1% sodium azide in PBS), cells were stained with anti-IL-4 (11B11) and anti-IFN-γ (XMG1.2) or isotype-matched control antibodies. All intracellular antibodies were from Biolegend. Data were collected on an LSRII (BD Biosciences) and analyzed using FlowJo software (FlowJo LLC, Ashland, OR).

Purified CD16/32 (Clone 93) (Biolegend) was used in all samples prior to the addition of Abs to block nonspecific Ab binding, except for samples in which FcγR3 expression was being assessed. In those cases, Fc block was not performed, and conjugated anti-CD16/CD32 (2.4G2) (BD Biosciences, San Jose, CA) was added to the surface stain master mix. As controls for FcγR3 staining and to control for the addition of conjugated 2.4G2 on all Fc receptors, cells were stained with unconjugated 2.4G2 Ab in order to block receptors and subsequently stained with conjugated 2.4G2. As a separate control, cells were stained with unconjugated 2.4G2 Ab and subsequently stained with an isotype-matched control (IgG2a, Biolegend).

For nuclear transcription factor staining, cells were surface stained as above, after which they were fixed overnight using the Foxp3 transcription factor staining buffer set (eBiosciences/ThermoFisher, San Diego, CA). The next day cells were washed, blocked with rat IgG, and stained with anti-PLZF (9E12) and RORγt (Q31-378) (BD). After staining, cells were washed, resuspended, and data were immediately collected on a LSRII flow cytometer (BD Bioscience) and analyzed with FlowJo software (FlowJo LLC).

Cell isolation and culture for ex vivo cytokine analysis

Splenocytes were enriched for CD4 T cells by depletion of CD8 (53-6.7), CD11b (M1/70), MHCII (M5-114) (BioX-cell, West Lebanon, NH) with anti-rat and anti-mouse IgG

magnetic beads (Qiagen, Hilden, Germany). After enrichment, cells were stained with anti-TCRβ, CD1d-tetramer/PBS57, and DAPI, and iNKT cells were purified by fluorescence activated cell sorting (FACS Aria III). Cell purity for all sorts was between 83 and 97%. After sorting, cells were placed in modified Click's culture medium (5% FBS, 2 mM glutamine, Pen/Strep, 50 μM 2-mercaptoethanol, 20 μg/mL gentamycin) and incubated on anti-CD3 (5 μg/mL) and anti-CD28 (1 μg/mL)-coated plates at 37 °C and 5% CO2. 72 h later, supernatants were harvested and analyzed via Milliplex assay, according to the manufacturer's instructions (EMD Millipore, Darmstadt, Germany). The milliplex kits used were the Mouse cytokine/chemokine magnetic bead panel followed by a custom kit containing GM-CSF, IFN-γ, IL-2, IL-4, IL-5, IL-10, IL-13, and IL-17.

Quantitative real-time PCR

Sorted iNKT cells were washed in cold PBS, after which cell pellets were snap frozen and kept at −80 °C until RNA was isolated. RNA isolation was performed using the RNeasy Micro kit according to the manufacturer's instructions (Qiagen, Hilden, Germany). cDNA was synthesized using Superscript III (ThermoFisher, San Diego, CA). *Mpz* and *Pcp4l-1* expression was evaluated by PCR using the gene-specific primers: Mpz forward 5′-CGGACAGGGA AATCTATGGTGC-3′, reverse 5′-TGGTAGCGCCAGG-TAAAAGAG-3′. Pcp4l-1 forward 5′-ATGAGCGAGCTT AACACCAAA-3′, reverse 5′- CTGCCAGGCTTCCCTT TTTC-3′ using cDNA derived from central nervous system tissue (a gift from D. Krementsov, University of Vermont). Expression of *Fcgr3*, *Sdhc*, and *Cfap126* was evaluated using Assay on Demand (AOD) Taqman probes (Life Technologies, Carlsbad, CA) according to the manufacturer's instructions. qPCR assay on demand (AOD) was run using the Perfecta qPCR SuperMix (Quanta Biosciences, Beverly MA). Samples were incubated with UNG SuperMIX at 45 °C for 5 m, then denatured initially at 95 °C for 3 m, followed by: 95 °C denaturation for 15 s, and a combined 60 °C annealing and extension step for 45 s for 40 cycles. Fold change was calculated by determining $2^{-\Delta\Delta CT}$ using mouse β-Actin as the endogenous control. Data were collected on an ABI Prism 7900HT Sequence Detection System.

Statistics

All animal experiments were conducted in a non-randomized and non-blinded fashion. One-way ANOVA, two-way ANOVA, or unpaired *t*-tests were used where appropriate. ANOVA post-hoc analysis comparisons were made using Dunnett's test, Sidak's multiple comparisons

test, or Holm–Sidak's multiple comparisons test where appropriate. In all cases, tests were considered significant when $p \leq 0.05$. All groups were shown to have similar variance in distribution. Sample size estimates were based on previous experience. In Fig. 2b, three mice were excluded from the analysis due to poor αGalCer injections. When data were combined from multiple different experiments, data were first normalized to the C57BL/6 reference strain in each experiment. Normalization was accomplished by dividing each data point in an experiment by the average of the C57BL/6 response in that experiment. All statistical analysis was performed using GraphPad Prism (GraphPad Software, San Diego, CA).

Compliance with ethical standards

Conflict of interest The authors declare that they have no conflict of interest.

References

1. Godfrey DI, Rossjohn J. New ways to turn on NKT cells. J Exp Med. 2011;208:1121–5.
2. Gumperz JE, Brenner MB. CD1-specific T cells in microbial immunity. Curr Opin Immunol. 2001;13:471–8.
3. Behar SM, Porcelli SA. CD1-restricted T cells in host defense to infectious diseases. Curr Top Microbiol Immunol. 2007;314:215–50.
4. Spada FM, Koezuka Y, Porcelli SA. CD1d-restricted recognition of synthetic glycolipid antigens by human natural killer T cells. J Exp Med. 1998;188:1529–34.
5. Pellicci DG, Patel O, Kjer-Nielsen L, Pang SS, Sullivan LC, Kyparissoudis K, et al. Differential recognition of CD1d-alpha-galactosyl ceramide by the V beta 8.2 and V beta 7 semi-invariant NKT T cell receptors. Immunity. 2009;31:47–59.
6. Kawano T, Cui J, Koezuka Y, Toura I, Kaneko Y, Motoki K, et al. CD1d-restricted and TCR-mediated activation of valpha14 NKT cells by glycosylceramides. Science. 1997;278:1626–9.
7. Wieland Brown LC, Penaranda C, Kashyap PC, Williams BB, Clardy J, Kronenberg M, et al. Production of alpha-galactosylceramide by a prominent member of the human gut microbiota. PLoS Biol. 2013;11:e1001610.
8. Borg NA, Wun KS, Kjer-Nielsen L, Wilce MC, Pellicci DG, Koh R, et al. CD1d-lipid-antigen recognition by the semi-invariant NKT T-cell receptor. Nature. 2007;448:44–9.
9. Kawano T, Cui J, Koezuka Y, Toura I, Kaneko Y, Sato H, et al. Natural killer-like nonspecific tumor cell lysis mediated by specific ligand-activated Valpha14 NKT cells. Proc Natl Acad Sci USA. 1998;95:5690–3.
10. Takahashi T, Nieda M, Koezuka Y, Nicol A, Porcelli SA, Ishikawa Y, et al. Analysis of human V alpha 24+ CD4+ NKT cells activated by alpha- glycosylceramide-pulsed monocyte-derived dendritic cells. J Immunol. 2000;164:4458–64.
11. Koch M, Stronge VS, Shepherd D, Gadola SD, Mathew B, Ritter G, et al. The crystal structure of human CD1d with and without alpha-galactosylceramide. Nat Immunol. 2005;6:819–26.
12. Yoshimoto T, Paul WE. CD4pos, NK1.1pos T cells promptly produce interleukin 4 in response to in vivo challenge with anti-CD3. J Exp Med. 1994;179:1285–95.
13. Coquet JM, Chakravarti S, Kyparissoudis K, McNab FW, Pitt LA, McKenzie BS, et al. Diverse cytokine production by NKT cell subsets and identification of an IL-17-producing CD4-NK1.1- NKT cell population. Proc Natl Acad Sci USA. 2008;105:11287–92.
14. Gumperz JE, Miyake S, Yamamura T, Brenner MB. Functionally distinct subsets of CD1d-restricted natural killer T cells revealed by CD1d tetramer staining. J Exp Med. 2002;195:625–36.
15. Sada-Ovalle I, Chiba A, Gonzales A, Brenner MB, Behar SM. Innate invariant NKT cells recognize Mycobacterium tuberculosis-infected macrophages, produce interferon-gamma, and kill intracellular bacteria. PLoS Pathog. 2008;4:e1000239.
16. Kitamura H, Iwakabe K, Yahata T, Nishimura S, Ohta A, Ohmi Y, et al. The natural killer T (NKT) cell ligand alpha-galactosylceramide demonstrates its immunopotentiating effect by inducing interleukin (IL)-12 production by dendritic cells and IL-12 receptor expression on NKT cells. J Exp Med. 1999;189:1121–8.
17. Hermans IF, Silk JD, Gileadi U, Salio M, Mathew B, Ritter G, et al. NKT cells enhance CD4+ and CD8+ T cell responses to soluble antigen in vivo through direct interaction with dendritic cells. J Immunol. 2003;171:5140–7.
18. Eberl G, MacDonald HR. Selective induction of NK cell proliferation and cytotoxicity by activated NKT cells. Eur J Immunol. 2000;30:985–92.
19. Carnaud C, Lee D, Donnars O, Park SH, Beavis A, Koezuka Y, et al. Cutting edge: cross-talk between cells of the innate immune system: NKT cells rapidly activate NK cells. J Immunol. 1999;163:4647–50.
20. Borg ZD, Benoit PJ, Lilley GW, Aktan I, Chant A, DeVault VL, et al. Polymorphisms in the CD1d promoter that regulate CD1d gene expression are associated with impaired NKT cell development. J Immunol. 2014;192:189–99.
21. Chen YG, Tsaih SW, Serreze DV. Genetic control of murine invariant natural killer T-cell development dynamically differs dependent on the examined tissue type. Genes Immun. 2012;13:164–74.
22. Rymarchyk SL, Lowenstein H, Mayette J, Foster SR, Damby DE, Howe IW, et al. Widespread natural variation in murine natural killer T-cell number and function. Immunology. 2008;125:331–43.
23. Lee YJ, Wang H, Starrett GJ, Phuong V, Jameson SC, Hogquist KA. Tissue-specific distribution of iNKT cells impacts their cytokine response. Immunity. 2015;43:566–78.
24. Hammond KJ, Pellicci DG, Poulton LD, Naidenko OV, Scalzo AA, Baxter AG, et al. CD1d-restricted NKT cells: an interstrain comparison. J Immunol. 2001;167:1164–73.
25. Gombert JM, Herbelin A, Tancrede-Bohin E, Dy M, Carnaud C, Bach JF. Early quantitative and functional deficiency of NK1+ -like thymocytes in the NOD mouse. Eur J Immunol. 1996;26:2989–98.
26. Benoit P, Sigounas VY, Thompson JL, van Rooijen N, Poynter ME, Wargo MJ, et al. The role of CD1d-restricted NKT cells in the clearance of Pseudomonas aeruginosa from the lung is

dependent on the host genetic background. Infect Immun. 2015;83:2557–65.

27. Tupin E, Benhnia MR, Kinjo Y, Patsey R, Lena CJ, Haller MC, et al. NKT cells prevent chronic joint inflammation after infection with Borrelia burgdorferi. Proc Natl Acad Sci USA. 2008;105:19863–8.

28. Olson CM Jr, Bates TC, Izadi H, Radolf JD, Huber SA, Boyson JE, et al. Local production of IFN-gamma by invariant NKT cells modulates acute Lyme carditis. J Immunol. 2009;182:3728–34.

29. Jordan MA, Fletcher JM, Pellicci D, Baxter AG. Slamf1, the NKT cell control gene Nkt1. J Immunol. 2007;178:1618–27.

30. Esteban LM, Tsoutsman T, Jordan MA, Roach D, Poulton LD, Brooks A, Naidenko OV, Sidobre S, Godfrey DI, Baxter AG. Genetic control of NKT cell numbers maps to major diabetes and lupus loci. J Immunol. 2003;171:2873–8.

31. Aktan I, Chant A, Borg ZD, Damby DE, Leenstra PC, Lilley GW, et al. Slam haplotypes modulate the response to lipopoly-saccharide in vivo through control of NKT cell number and function. J Immunol. 2010;185:144–56.

32. Fletcher JM, Jordan MA, Snelgrove SL, Slattery RM, Dufour FD, Kyparissoudis K, et al. Congenic analysis of the NKT cell control gene Nkt2 implicates the peroxisomal protein Pxmp4. J Immunol. 2008;181:3400–12.

33. Wesley JD, Tessmer MS, Paget C, Trottein F, Brossay LA. Y chromosome-linked factor impairs NKT development. J Immunol. 2007;179:3480–7.

34. Zhang F, Liang Z, Matsuki N, Van Kaer L, Joyce S, Wakeland EK, et al. A murine locus on chromosome 18 controls NKT cell homeostasis and the cell differentiation. J Immunol. 2003;171:4613–20.

35. Araujo LM, Puel A, Gouarin C, Hameg A, Mevel JC, Koezuka Y, et al. NKT lymphocyte ontogeny and function are impaired in low antibody- producer Biozzi mice: gene mapping in the interval-specific congenic strains raised for immunomodulatory genes. Int Immunol. 2000;12:1613–22.

36. Rocha-Campos AC, Melki R, Zhu R, Deruytter N, Damotte D, Dy M, et al. Genetic and functional analysis of the Nkt1 locus using congenic NOD mice: improved Valpha14-NKT cell performance but failure to protect against type 1 diabetes. Diabetes. 2006;55:1163–70.

37. Griewank K, Borowski C, Rietdijk S, Wang N, Julien A, Wei DG, et al. Homotypic interactions mediated by Slamf1 and Slamf6 receptors control NKT cell lineage development. Immunity. 2007;27:751–62.

38. Wandstrat AE, Nguyen C, Limaye N, Chan AY, Subramanian S, Tian XH, et al. Association of extensive polymorphisms in the SLAM/CD2 gene cluster with murine lupus. Immunity. 2004;21:769–80.

39. Edberg JC, Langefeld CD, Wu J, Moser KL, Kaufman KM, Kelly J, et al. Genetic linkage and association of Fc gamma receptor IIIA (CD16A) on chromosome 1q23 with human systemic lupus erythematosus. Arthritis Rheum. 2002;46:2132–40.

40. Morel L, Blenman KR, Croker BP, Wakeland EK. The major murine systemic lupus erythematosus susceptibility locus, Sle1, is a cluster of functionally related genes. Proc Natl Acad Sci USA. 2001;98:1787–92.

41. Baxter AG, Kinder SJ, Hammond KJ, Scollay R, Godfrey DI. Association between alphabetaTCR+CD4-CD8- T-cell deficiency and IDDM in NOD/Lt mice. Diabetes. 1997;46:572–82.

42. Cardell SL. The natural killer T lymphocyte: a player in the complex regulation of autoimmune diabetes in non-obese diabetic mice. Clin Exp Immunol. 2006;143:194–202.

43. Esteban LM, Tsoutsman T, Jordan MA, Roach D, Poulton LD, Brooks A, et al. Genetic control of NKT cell numbers maps to major diabetes and lupus loci. J Immunol. 2003;171:2873–8.

44. Jordan MA, Fletcher JM, Jose R, Chowdhury S, Gerlach N, Allison J, et al. Role of SLAM in NKT cell development revealed by transgenic complementation in NOD mice. J Immunol. 2011;186:3953–65.

45. Lee YJ, Holzapfel KL, Zhu J, Jameson SC, Hogquist KA. Steady-state production of IL-4 modulates immunity in mouse strains and is determined by lineage diversity of iNKT cells. Nat Immunol. 2013;14:1146–54.

46. Heng TS, Painter MW, Immunological Genome Project Consortium. The Immunological Genome Project: networks of gene expression in immune cells. Nat Immunol. 2008;9:1091–4.

47. Kim HY, Kim S, Chung DH. FcgammaRIII engagement provides activating signals to NKT cells in antibody-induced joint inflammation. J Clin Invest. 2006;116:2484–92.

48. Nieuwenhuis EE, Matsumoto T, Exley M, Schleipman RA, Glickman J, Bailey DT, et al. CD1d-dependent macrophage-mediated clearance of Pseudomonas aeruginosa from lung. Nat Med. 2002;8:588–93.

49. Stevenson MM, Kondratieva TK, Apt AS, Tam MF, Skamene E. In vitro and in vivo T cell responses in mice during broncho-pulmonary infection with mucoid Pseudomonas aeruginosa. Clin Exp Immunol. 1995;99:98–105.

50. Jordan MA, Fletcher J, Baxter AG. Genetic control of NKT cell numbers. Immunol Cell Biol. 2004;82:276–84.

51. Godfrey DI, Kinder SJ, Silvera P, Baxter AG. Flow cytometric study of T cell development in NOD mice reveals a deficiency in alphabetaTCR+CDR-CD8- thymocytes. J Autoimmun. 1997;10:279–85.

52. Nimmerjahn F, Ravetch JV. Fc-receptors as regulators of immunity. Adv Immunol. 2007;96:179–204.

53. Dreos R, Ambrosini G, Groux R, Cavin Perier R, Bucher P. The eukaryotic promoter database in its 30th year: focus on non-vertebrate organisms. Nucleic Acids Res. 2017;45(D1):D51–D5.

54. Park-Min KH, Serbina NV, Yang W, Ma X, Krystal G, Neel BG, et al. FcgammaRIII-dependent inhibition of interferon-gamma responses mediates suppressive effects of intravenous immune globulin. Immunity. 2007;26:67–78.

55. Araujo LM, Chauvineau A, Zhu R, Diem S, Bourgeois EA, Levescot A, et al. Cutting edge: intravenous Ig inhibits invariant NKT cell-mediated allergic airway inflammation through FcgammaRIIIA-dependent mechanisms. J Immunol. 2011;186:3289–93.

56. Sandor M, Galon J, Takacs L, Tatsumi Y, Mueller AL, Sautes C, et al. An alternative Fc gamma-receptor ligand: potential role in T-cell development. Proc Natl Acad Sci USA. 1994;91:12857–61.

57. Rodewald HR, Moingeon P, Lucich JL, Dosiou C, Lopez P, Reinherz EL. A population of early fetal thymocytes expressing Fc gamma RII/III contains precursors of T lymphocytes and natural killer cells. Cell. 1992;69:139–50.

58. Shores E, Flamand V, Tran T, Grinberg A, Kinet JP, Love PE. Fc epsilon RI gamma can support T cell development and function in mice lacking endogenous TCR zeta-chain. J Immunol. 1997;159:222–30.

59. Flamand V, Shores EW, Tran T, Huang K, Lee E, Grinberg A, et al. Delayed maturation of CD4- CD8- Fc gamma RII/III+ T and natural killer cell precursors in Fc epsilon RI gamma transgenic mice. J Exp Med. 1996;184:1725–35.

60. Georgiev H, Ravens I, Benarafa C, Forster R, Bernhardt G. Distinct gene expression patterns correlate with developmental and functional traits of iNKT subsets. Nat Commun. 2016;7:13116.

61. Renkema GH, Wortmann SB, Smeets RJ, Venselaar H, Antoine M, Visser G, et al. SDHA mutations causing a multisystem mitochondrial disease: novel mutations and genetic overlap with hereditary tumors. Eur J Hum Genet. 2015;23:202–9.

62. Bader E, Migliorini A, Gegg M, Moruzzi N, Gerdes J, Roscioni SS, et al. Identification of proliferative and mature beta-cells in the islets of Langerhans. Nature. 2016;535:430–4.

63. Frias AB, Jr, Buechel HM, Neupane A, D'Cruz LM. Invariant natural killer T-cell development and function with loss of microRNA-155. Immunology. 2017;153:238–45.

64. Burocchi A, Pittoni P, Tili E, Rigoni A, Costinean S, Croce CM, et al. Regulated expression of miR-155 is required for iNKT cell development. Front Immunol. 2015;6:140.

65. Fedeli M, Riba M, Garcia Manteiga JM, Tian L, Vigano V, Rossetti G, et al. miR-17 approximately 92 family clusters control iNKT cell ontogenesis via modulation of TGF-beta signaling. Proc Natl Acad Sci USA. 2016;113:E8286–E95.

66. Castellano L, Stebbing J. Deep sequencing of small RNAs identifies canonical and non-canonical miRNA and endogenous siRNAs in mammalian somatic tissues. Nucleic Acids Res. 2013;41:3339–51.

67. Meunier J, Lemoine F, Soumillon M, Liechti A, Weier M, Guschanski K, et al. Birth and expression evolution of mammalian microRNA genes. Genome Res. 2013;23:34–45.

68. Aken BL, Ayling S, Barrell D, Clarke L, Curwen V, Fairley S, et al. The Ensembl gene annotation system. Database. 2016;2016:baw093.